A 3-D, Adaptive, Fully Implicit, Numerical Model of Hydraulic Fracturing Process, Fracture Cleanup, and Relevant Thermo-Elastic Computations

Doctor of Philosophy in Petroleum Engineering Dissertation Proposal

by

Sarinya Charoenwongsa

A 3-D, Adaptive, Fully Implicit, Numerical Model of Hydraulic Fracturing Process, Fracture Cleanup, and Relevant Thermo-Elastic Computations

Doctor of Philosophy in Petroleum Engineering Dissertation Proposal

by

Sarinya Charoenwongsa

The attached document is a Doctor of Philosophy dissertation proposal for Sarinya Charoenwongsa. It contains a detailed outline of the proposed thesis work, objectives for the project and a summary of completed class work. Your permission and agreement to proceed with the project as outlined in this document is requested.

Date: _____ Submitted by: _____ Sarinya Charoenwongsa

Date:_____ Approved by: _____ Advisor, Dr. Jennifer Miskimins

Date: _____ Approved by: _____ Advisor, Dr. Hossein Kazemi

Date: _____ Approved by: _____ Dr. John Curtis

Date: _____ Approved by: _____ Dr. Erdal Ozkan

Date: _____ Approved by: _____ Dr. Yu-Shu Wu

Date: _____ Approved by: _____ Dr. Ugur Ozbay

INTRODUCTION

This dissertation aims to provide further understanding of formation/fracture damages and gel cleanup mechanisms. These mechanisms are responsible for the effectiveness of tight gas hydraulic fracturing. Based on previous laboratory measurements, mathematical analyses and field case histories[1-4], various issues affecting these mechanisms have been identified and are summarized below:

Classical Issues:

- Formation damages
  - Water block and excessive leakoff
- Fracture damages
  - Gel residue: gel filter cake, unbroken gel
  - Proppant damages: compaction, crushing and embedment

Current Issues:

- Geomechanical and thermal effects
  - Creating new microfractures near the faces of the hydraulic fracture
  - Reopening (or dilating) existing closed natural fractures

Related Issues:

- Multi-phase flow effects, reservoir heterogeneity, rheology of polymer gel, gel degradation, pressure drawdown and non-Darcy flow effects

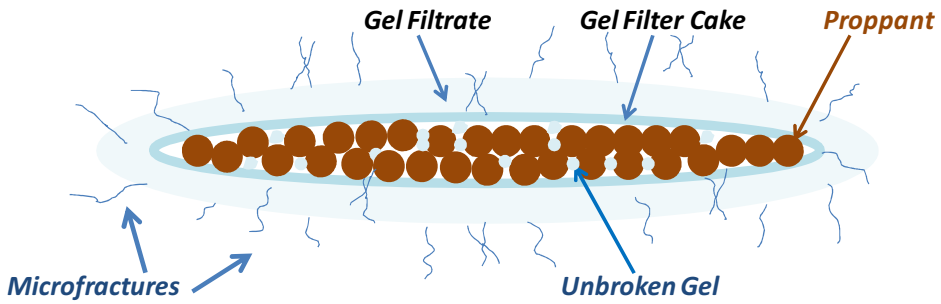

Figure 1. Formation/fracture damages and geomechanical and thermal effects.

OBJECTIVES

Research Goal:

- Develop a robust numerical model for the hydraulic fracturing process that incorporates fracture cleanup and relevant thermo-elastic computations.

Dissertation Objectives:

- Assess the state of the following:
    - Mathematical and physical modeling
    - Applied numerical simulation techniques
- Develop a 3-D adaptive, fully implicit, numerical model for the hydraulic fracturing process with fracture cleanup and relevant thermo-elastic calculations. This model will account for fracture propagation, fluid leakoff, fracture closure, fracture cleanup, multiphase flow effects (gravity-capillary interaction, relative permeability), reservoir heterogeneity, rheology of polymer gel, gel degradation, non-Darcy and stress alterations near the fracture face (geomechanics) and heat transfer.
- Validate the new code.
- Conduct sensitivity studies to understand the factors affecting hydraulic fracturing process and fracture cleanup.
- Propose ideas to improve fracture cleanup.

WORK SCOPE

It is intended to extend the numerical model previously developed[4] to a more stable numerical solution (i.e. fully implicit approach vs. partially implicit approach) that accounts for multiphase flow effects (gravity-capillary interaction, relative permeability), reservoir heterogeneity, rheology of polymer gel, gel degradation, non-Darcy flow and stress alterations near the fracture face (geomechanics) and heat transfer. This model will be useful to simulate formation damages especially water block affecting the cleanup process in tight gas reservoirs. The following summarizes the features of the proposed and previous numerical models.

Table 1 Summary of the Features of Proposed and Previous Numerical Models

Features	Model		Remarks
	(previous)[4]	(proposed)	for the proposed model
Multiphase Darcy Flow			
Relative Permeability	●	●	Water Block, Excessive Leakoff
Capillary Pressure	●	●	
Gravity	●	●	-
Fluid Properties			
Newtonian	●	●	-
Non-Newtonian	●	●	Gel Residue
Matrix Properties			
Heterogeneity		●	-
Porosity, Permeability		●	Geomechanics & Phase Change
Hydraulic Fracture Properties			
Porosity, Permeability		●	Proppant Damages
Calculation			
Sequential Partially Implicit (IMPES)	●	●	-
Sequential Implicit		●	-
Fully Implicit		●	-
Non-Darcy Flow		●	-
Geomechanical Effects		●	-
Thermal Effects		●	-

OUTLINE OF WORK

- Perform literature search on
    - Formation and fracture damage mechanisms affecting the effectiveness of the fracture cleanup process; and,
    - Analytical and numerical models related to hydraulic fracturing, fracture cleanup and reservoir modeling.
- Develop an adaptive implicit fluid flow model for the fracture-reservoir system.
    - 3-D model for gas-brine, 3-components system to include polymer gel, filtrate and gel breaker; and,
    - Account for multiphase flow, reservoir heterogeneity, rheology of polymer gel, gel degradation and non-Darcy flow effects
- Develop a geomechanical model to account for effects of stress alterations near the fracture face (geomechanics) and heat transfer during the hydraulic fracturing process.
    - Fracture propagation and leakoff model (fracture module); and,
    - Geomechanics and flow model (reservoir module)
- Write the dissertation.

PROJECT STATUS

Governing equations have been developed for the two main modules: a) fracture module (fracture propagation and leakoff model) and b) reservoir module (geomechanics and flow model). The first version of the reservoir module has been coded. This code considers the effects of temperature, pore pressure, rock displacement, relative permeability, capillary pressure and gravity segregation. The preliminary results for water flooding example are provided at the end of this report.

Timetable

This project is a PhD level project and is set to span three years. **Table 2** shows the progress to date and proposed plan.

Table 2. Planned Timeline

Task	2008				2009				2010			
	Q1	Q2	Q3	Q4	Q1	Q2	Q3	Q4	Q1	Q2	Q3	Q4
Literature Review												
- Geomechanics and Flow Models												
- Fracture Propagation Models												
- Formation/ Fracture Damage and Fracture Cleanup Issues												
Model Development												
- Geomechanics and Flow Modeling Foundation Code												
- Hydraulic Fracture Modeling with Fully Implicit Flow Model												
(Formation/Fracture Damages, Geomechanics and Thermal Effects)												
- Model Validation & Sensitivity Studies												
Documentation												
-Dissertation												

MATHEMATICAL MODEL

Model Description

The system to be modeled includes rock matrix, a single fracture and a single vertical well. The rock matrix consists of reservoir layers (porous media) and overlying and underlying shale layers (non-porous media). Fluids in the system include gas and water with three components (e.g. gel, gel breaker and filtrate), existing in water phase. The vertical well will be used for both injection and production depending on the stage of the hydraulic fracturing process. Since the system is symmetric, only a quarter of this system will be modeled. The schematic of this system is illustrated in **Figure 2**.

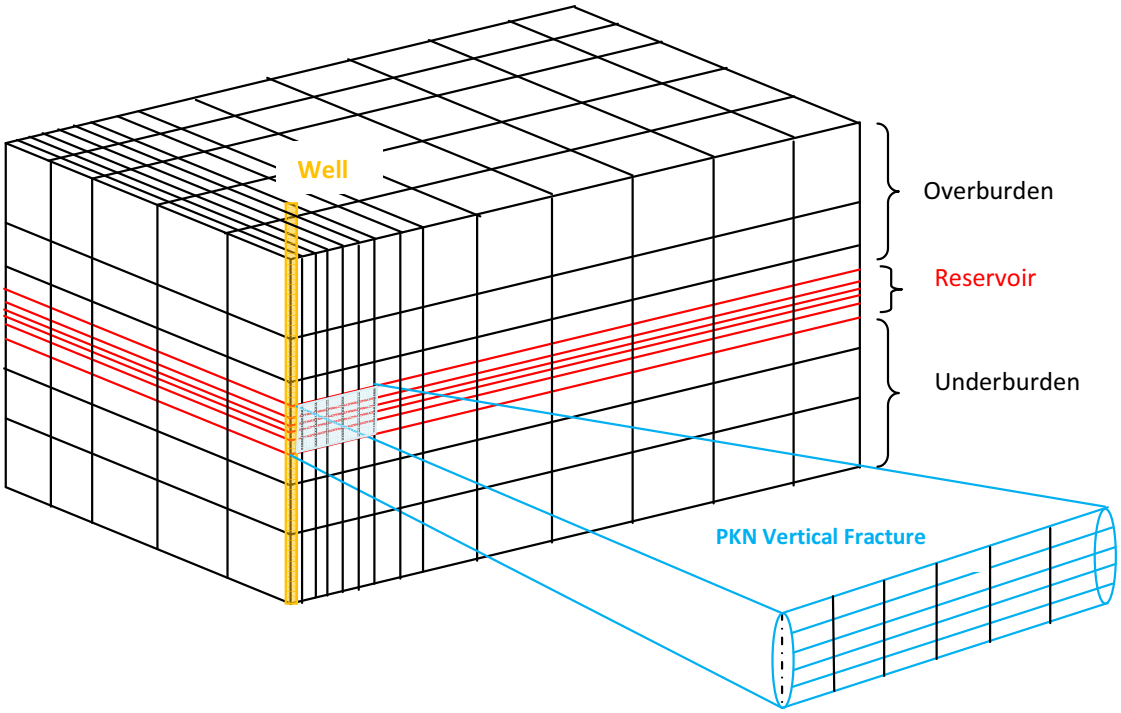

Figure 2. Hydraulically fractured reservoir system.

Model Development

Two mathematical models have been developed to simulate the physical processes involved in the hydraulic fracturing process and fracture cleanup performed in a tight gas reservoir. The first model is a fracture propagation and leakoff model (fracture module) and the second one is a geomechanics and flow model (reservoir module). These mathematical models are built based on the governing equations defining physical laws, including conservation of mass, momentum and energy, and constitutive laws, such as porothermoelasticity theory.

Fracture Propagation and Leakoff Model (Fracture Module)

A fracture propagation and leakoff model is used to describe the physical phenomena controlling fracture growth and fracture closure during the injection and shut-in periods (see **Figure 3**.)

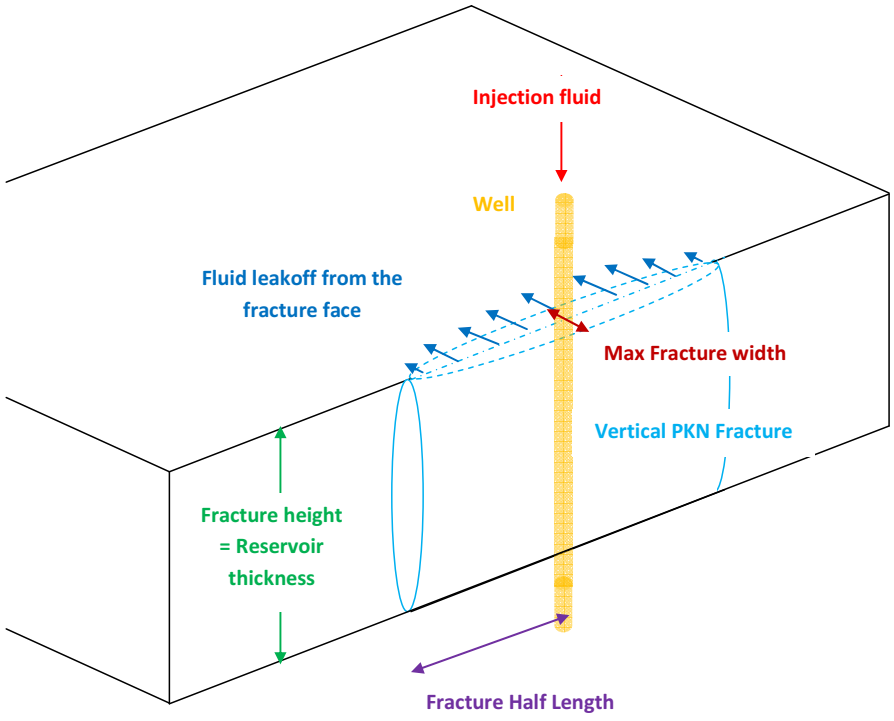

Figure 3. Fracture geometry and 1-D linear leakoff behavior.

Inherited assumptions and governing equations for the fracture propagation and leakoff model are as follows:

Assumptions

- A vertical well is hydraulically stimulated in a tectonically relaxed area where the vertical stress is the maximum in-situ stress. Thus, a hydraulic fracture will have a vertical orientation and propagate in the direction of the maximum horizontal in-situ stress, perpendicular to the minimum horizontal in-situ stress;
- The simulation axes are fixed in the directions of the maximum (x-axis) and minimum (y-axis) stresses in the horizontal plane, and in the direction of the vertical stresses for the z-direction;
- A PKN vertical fracture is created and fully contained within the pay zone. This fracture is long and constant-height with two wings. The flow rate in each wing is a half of well injection rate (q_i);
- During injection, the flow behavior of leakoff can be considered as 1-D linear; and;
- Fracture tip/toughness/mechanics effects are ignored.

Governing Equations

The following governing equations are derived in a similar manner as the previous study[4]. These equations are developed from three major equations: mass balance equation and 1-D leakoff model proposed by Carter[5] (Eq.1) and the fracture width equation proposed by England and Green[6] (Eqs.2 and 3).

$$\frac{q_i}{2} = 2\int_0^t \frac{C_L}{\sqrt{t-\lambda}} \frac{dA_f}{d\lambda} d\lambda + \overline{w}_f \frac{dA_f}{dt} \quad (1)$$

$$\overline{w}_f = \left(\frac{\pi}{4}\right)^2 w_{f,max} \quad (2)$$

$$w_{f,max} = \frac{2(1-\upsilon)(P_f - \sigma_h)L_f}{G} \quad (3)$$

A half of the first term in the right-handed side of Eq. 1 will be used as a flow source term for the reservoir node(s) adjacent to the fracture during injection and Eqs.2 and 3 will be used to estimate the average fracture width during injection and shut-in periods.

Geomechanics and Flow Model (Reservoir Module)

A geomechanics and flow model is used to describe fluid flow, heat transfer and rock deformation in both the fracture and rock matrix. The governing equations are developed based on conservation of mass, momentum and energy, and porothermoelasticity theory. We have extended the governing equations presented by Jaeger[7] to multiphase flow system and also modified a set of conservation equations to properly couple the fluid flow governing equations with the geomechanics and thermal ones specifically. Inherited assumptions, governing equations and constitutive relations are presented as follows:

Assumptions

- Fluids flow in the fracture and reservoir matrix under pressure, viscous and gravity forces according to Darcy's law;
- The interference between the phases during flowing through the fracture and reservoir matrix can be described via relative permeability and capillary pressure functions;
- The system consists of two fluid phases (gas and water) and the presence of filtrate, gel and gel breaker in the aqueous phase;
- Convective heat transfer occurs simultaneously with fluid flow, while conductive heat transfer occurs in reservoir and surrounding rocks;
- Rock deformation behaves as a perfect elastic media (linear, reversible and non-retarded mechanical behavior) with small strains;
- The mechanical behavior of the rock matrix responds to changes in temperature, and effective stress and strain. The mechanical responses include changes in volumetric strain with accompanying changes in both matrix porosity and permeability;
- The mechanical behavior of the propped fracture responds to changes in closure stress with accompanying changes in both fracture (proppant) porosity and permeability;
- Initially, fluid and solid components are in gravity-capillarity equilibrium; and,
- The entire fracture is filled with a uniform, preselected and designed proppant concentration during shut-in and fracture cleanup.

Governing Equations

The governing equations for the geomechanics and flow model are given by Eqs.4-10.

Global Pore Pressure Equation:

$$\nabla \cdot \{k\lambda_t[\nabla P_g - (f_w\gamma_w + f_g\gamma_g)\nabla D - f_w\nabla P_{cwg}]\} + \hat{q}_t = \phi c_t \frac{\partial P_g}{\partial t} - \alpha_p \frac{\partial(\nabla\cdot\vec{u})}{\partial t} - (S_w\alpha_{T,w} + S_g\alpha_{T,g})\frac{\partial T}{\partial t} \tag{4}$$

Displacement Equation:

$$G\nabla^2\vec{u} + (G+\lambda)\nabla(\nabla\cdot\vec{u}) = -\alpha_p\{\nabla P_g - (f_w\gamma_w + f_g\gamma_g)\nabla D - f_w\nabla P_{cwg}\} - 3\alpha_{T,b}K_b\nabla T \tag{5}$$

Temperature Equation:

$$\nabla \cdot \{k\lambda_t[(\rho_w c_{p,w} f_w + \rho_g c_{p,g} f_g)\nabla P_g - (\rho_w c_{p,w} f_w \gamma_w + \rho_g c_{p,g} f_g \gamma_g)\nabla D - \rho_w c_{p,w} f_w \nabla P_{cwg}]T\}$$
$$+\nabla \cdot (k_T \nabla T) + \rho_i c_{p,i}\hat{q}_i(T_i - T_{ref}) = \{\phi(\rho_w c_{p,w} S_w + \rho_g c_{p,g} S_g) + (1-\phi)\rho_s c_{p,s}\}\frac{\partial T}{\partial t} - 3\alpha_{T,b}K_b T_{ref}\frac{\partial(\nabla\cdot\vec{u})}{\partial t} \tag{6}$$

Water Saturation Equation

$$\nabla \cdot \{k\lambda_w[\nabla P_g - \gamma_w \nabla D - \nabla P_{cwg}]\} + \hat{q}_w = \phi \left[(c_w + c_\phi)S_w \frac{\partial P_g}{\partial t} + \frac{\partial S_w}{\partial t}\right] \tag{7}$$

Concentration Equations

$$\nabla \cdot \{k\lambda_w[(\nabla P_g - \gamma_w \nabla D - \nabla P_{cwg})C_1]\} + \hat{q}_w C_1 = \phi \left[(c_w + c_\phi)S_w C_1 \frac{\partial P_g}{\partial t} + \frac{\partial(S_w C_1)}{\partial t}\right] \tag{8}$$

$$\nabla \cdot \{k\lambda_w[(\nabla P_g - \gamma_w \nabla D - \nabla P_{cwg})C_2]\} + \hat{q}_w C_2 = \phi \left[(c_w + c_\phi)S_w C_2 \frac{\partial P_g}{\partial t} + \frac{\partial(S_w C_2)}{\partial t}\right] \tag{9}$$

$$\nabla \cdot \{k\lambda_w[(\nabla P_g - \gamma_w \nabla D - \nabla P_{cwg})C_3]\} + \hat{q}_w C_3 = \phi \left[(c_w + c_\phi)S_w C_3 \frac{\partial P_g}{\partial t} + \frac{\partial(S_w C_3)}{\partial t}\right] \tag{10}$$

Constitutive Relations

The constitutive relations for the geomechanics and flow model are given by Eqs.11-28.

Flow Properties

Fluid Gravity: $\gamma_\varphi = \frac{\rho_\varphi}{144}$ (11)

Total compressibility: $c_t = c_\phi + S_w c_w + S_g c_g$ (12)

Gas compressibility: $c_g = \frac{1}{P_g} - \frac{1}{z}\frac{\partial z}{\partial P_g}$ (13)

Mobility Ratio: $\lambda_\varphi = \frac{k_{r\varphi}}{\mu_\varphi}$ (14)

Total Mobility Ratio: $\lambda_t = \lambda_w + \lambda_g$ (15)

Phase Fractional Flow: $f_\varphi = \frac{\lambda_\varphi}{\lambda_t}$ (16)

Relative Permeability: $k_{r\varphi} = k_{r\varphi}(S_w)$ (17)

Capillary Pressure: $P_{cgw} = P_{cgw}(S_w)$ (18)

Saturation Constraints: $S_w + S_g = 1$ (19)

Linear Thermal Expansion Coefficient: $\alpha_{t,b} = \phi\left(S_w\alpha_{t,w} + S_g\alpha_{t,g}\right) + (1-\phi)\alpha_{t,s}$ (20)

Geomechanical Properties

Strain-Displacement Relation:

$$\varepsilon_{ij} = \frac{1}{2}\left(\frac{\partial u_i}{\partial x_j} + \frac{\partial u_j}{\partial x_i}\right) \quad (21)$$

Volumetric Strain:

$$\varepsilon_v = \sum \delta_{ij}\varepsilon_{ij} = \nabla \cdot \vec{u} \quad (22)$$

Extended Hooke's Law (including pore pressure and temperature effects):

$$\sigma_{ij} = 2G\varepsilon_{ij} + \lambda\varepsilon_v\delta_{ij} + \alpha_p P\delta_{ij} + 3\alpha_{T,b}K_b(T - T_{ref})\delta_{ij} \quad (23)$$

$$\Delta\sigma_{ij} = 2G\Delta\varepsilon_{ij} + \lambda\Delta\varepsilon_v\delta_{ij} + \alpha_p\Delta P\delta_{ij} + 3\alpha_{T,b}K_b\Delta T\delta_{ij} \quad (24)$$

Matrix Porosity[8]*:*

$$\phi = \phi_0 + (e^{-\varepsilon_v} - 1) \quad (25)$$

Matrix Permeability:

$$k = k(\varepsilon_v) \quad (26)$$

Fracture Porosity:

$$\phi_f = \phi_f(\sigma_h) \quad (27)$$

Fracture Permeability:

$$k_f = k_f(\sigma_h) \quad (28)$$

Initial and Boundary Conditions (See **Figure 4**)

Initial and boundary conditions for the geomechanics and flow model are provided as follows.

- Gravity-capillary pressure equilibrium at initial condition

$$\left(\nabla P_g - \left(f_w\gamma_w + f_g\gamma_g\right)\nabla D - f_w\nabla P_{cwg}\right)^0 = 0$$

- Given initial pore pressure, temperature, water saturation and concentration of gel, gel breaker and water

$$P(x,y,z,0) = P^0$$

$$T(x,y,z,0) = T^0$$
$$S_w(x,y,z,0) = S_w^0$$
$$C_1(x,y,z,0) = C_1^0$$
$$C_2(x,y,z,0) = C_2^0$$
$$C_3(x,y,z,0) = C_3^0$$

- Zero incremental displacement at initial condition

$$u(x,y,z,0) = 0$$
$$v(x,y,z,0) = 0$$
$$w(x,y,z,0) = 0$$

- Non-deformable bottom shale boundary

$$w(x,y,z,t)_{bottom\ boundary} = 0$$

- Non-deformable lateral reservoir boundaries (only for reservoir boundary not connected to a fracture)

$$u(x,y,z,t)_{lateral\ boundary} = 0$$
$$v(x,y,z,t)_{lateral\ boundary} = 0$$

- Deformable lateral reservoir boundaries (only for reservoir boundary adjacent to a fracture)

$$u(x,y,z,t)_{lateral\ boundary} = L_f(t)$$
$$v(x,y,z,t)_{lateral\ boundary} = \frac{\bar{w}_f}{2}(t)$$

- Deformable top shale boundaries

$$\left(\frac{\partial w(x,y,z,t)}{\partial z}\right)_{top\ boundary} = 0$$

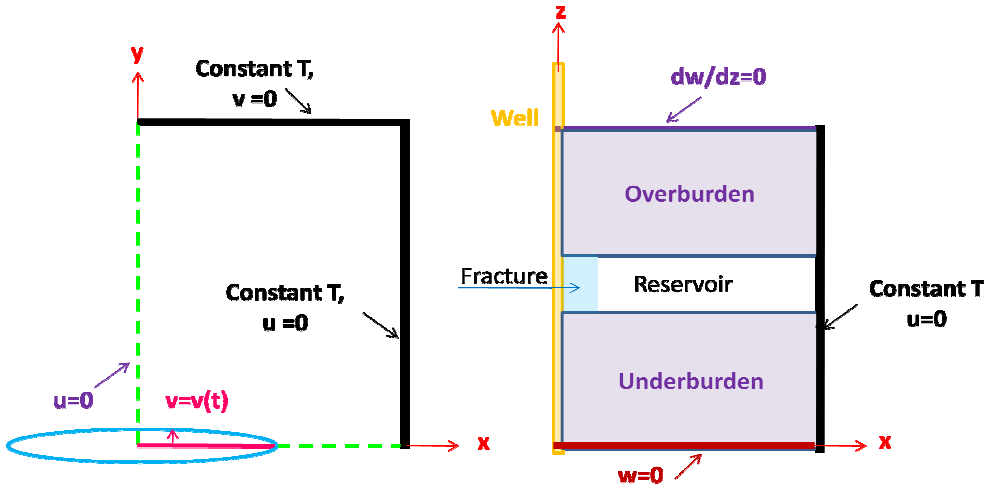

Figure 4. Boundary conditions: lateral boundary (left) and vertical boundary (right).

NUMERICAL FORMULATION AND SOLUTIONS

Fracture Propagation and Leakoff Model (Fracture Module)

Numerical Approximation

Eq.1 can be numerically approximated by Eq.29.

$$q_i = \left[2\sum_{j=1}^{n}\frac{C_L A_{f,j}}{\sqrt{t_n - t_{j-1}}}\right] + \frac{\bar{w}_f(t_n)A_{f,n}}{t_n - t_{n-1}} \tag{29}$$

Where subscripts j and n denote the grid index along lateral fracture propagation (x-direction) and the grid index of the last fracture segment, respectively.

Based on specified fracture pressure (P_f) and fracture grid length (ΔL), a corresponding average fracture width $(\bar{w}_f)$ can be readily calculated from Eqs.2 and 3. Substituting this calculated $\bar{w}_f$ in Eq.29, time used to create the fracture segment j (t_j) can be numerically solved using Newton-Raphson method. **Figure 5** shows how to solve for time corresponding to the second fracture segment created.

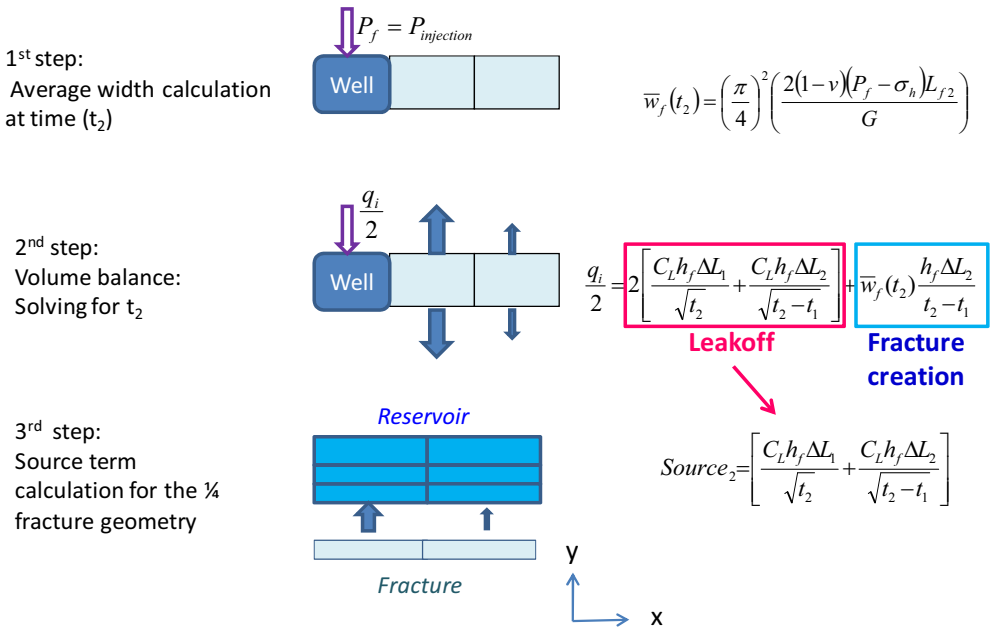

Figure 5. Example of numerical approximation of fracture propagation and leakoff model to solve for time corresponding to the second fracture segment created.

Geomechanics and Flow Model (Reservoir Module)

Solution Schemes

To solve this particular problem which consists of large, coupled systems of nonlinear, time-dependent partial differential equations (Eqs. 4-10), we have to find the most robust (unbreakable), computationally stable and efficient numerical solution method. In this study, the following numerical solution methods will be examined.

1. Implicit Pressure, Explicit Saturation (IMPES) -- sequential partially implicit method
2. Implicit Pressure, Implicit Saturation/Capillary Pressure -- sequential implicit method
3. Implicit Pressure, Implicit Saturation, and Implicit Transmissibility -- fully implicit method

IMPES and implicit pressure, implicit saturation/capillary pressure methods are sequential solution schemes. Using these methods, the global pore pressure equation is simultaneously solved for the pore pressure with geomechanics and temperature equations in a coupled manner, while the fluid saturation and concentration variables are computed sequentially based on pressure values previously solved from the pore pressure equation. Compared to *fully implicit methods*, *sequential methods* require smaller time step sizes and take shorter time to compute within a given time step. Its time step size limitation requires longer total time to compute for a whole simulation. However, smaller time steps provide a more accurate solution because of small numerical dispersion.

Implicit pressure, implicit saturation, and implicit transmissibility methods are simultaneous solution schemes. The global pore pressure and water saturation equations are simultaneously solved with geomechanics and temperature equations in a coupled manner, while concentration variables are computed sequentially based on pressure and fluid saturation values previously solved from the pore pressure and water saturation equations. Compared to *sequential methods*, *fully implicit methods* takes a longer time to compute within a given time step; however, it takes larger time step sizes. In addition, larger time steps provide a less accurate solution because of large numerical dispersion. However, *sequential implicit* and *fully implicit methods* should provide a more stable gravity segregation computation, which is very difficult to attain with *IMPES methods*.

The governing equations Eqs.4-10, can be written in partial differential forms for IMPES and implicit pressure implicit saturation/capillary pressure methods as follows in Eqs.29-42:

IMPES Method

Global Pore Pressure Equation

$$\nabla\cdot\left\{k\lambda_t^n\left[\nabla P_g^{n+1}-\left(f_w\gamma_w+f_g\gamma_g\right)^n\nabla D-\left(f_w\nabla P_{cwg}\right)^n\right]\right\}+\hat{q_t}=\phi c_t\frac{\partial P_g}{\partial t}-\alpha_p\frac{\partial(\nabla\cdot\vec{u})}{\partial t}-(S_w^n\alpha_{T,w}+S_g^n\alpha_{T,g})\frac{\partial T}{\partial t} \tag{29}$$

Displacement Equation

$$G\nabla^2\vec{u}^{n+1}+(G+\lambda)\nabla(\nabla\cdot\vec{u}^{n+1})+\overrightarrow{\gamma_b}=-\alpha_p\left\{\nabla P_g^{n+1}-\left(f_w\gamma_w+f_g\gamma_g\right)^n\nabla D-\left(f_w\nabla P_{cwg}\right)^n\right\}-3\alpha_{T,b}K_b\nabla T^{n+1} \tag{30}$$

Temperature Equation

$$\begin{aligned}&\nabla\cdot(k_T\nabla T^{n+1})+\nabla\cdot\left\{k\lambda_t^n\left[\left(\rho_w c_{p,w}f_w^n+\rho_g c_{p,g}f_g^n\right)\nabla P_g^{n+1}-\left(\rho_w c_{p,w}f_w^n\gamma_w^n+\rho_g c_{p,g}f_g^n\gamma_g^n\right)\nabla D-\rho_w c_{p,w}f_w^n\nabla P_{cwg}^n\right]T^{n+1}\right\}\\&+\rho_i c_{p,i}\hat{q}_i(T_i-T_{ref})=\left\{\phi^n\left(\rho_w c_{p,w}S_w^n+\rho_g c_{p,g}S_g^n\right)+(1-\phi)\rho_s c_{p,s}\right\}\frac{\partial T}{\partial t}-3\alpha_{T,b}K_bT_{ref}\frac{\partial(\nabla\cdot\vec{u}\ )}{\partial t}\end{aligned} \tag{31}$$

Water Saturation Equation

$$\nabla\cdot\left\{k\lambda_w^n\left[\nabla P_g^{(n+1)}-\gamma_w^n\nabla D-\nabla P_{cwg}^n\right]\right\}+\hat{q}_w=\phi^{(n+1)}\left[\left(c_w+c_\phi\right)S_w^n\frac{\partial P_g}{\partial t}+\frac{\partial S_w}{\partial t}\right] \tag{32}$$

Concentration Equations

$$\nabla\cdot\left\{k\lambda_w^n\left[\left(\nabla P_g^{(n+1)}-\gamma_w^n\nabla D-\nabla P_{cwg}^n\right)C_1^{n+1}\right]\right\}+\hat{q}_wC_1^{n+1}=\phi^{(n+1)}\left[\left(c_w+c_\phi\right)S_w^nC_1^{n+1}\frac{\partial P_g}{\partial t}+\frac{\partial(S_wC_1)}{\partial t}\right] \tag{33}$$

$$\nabla\cdot\left\{k\lambda_w^n\left[\left(\nabla P_g^{(n+1)}-\gamma_w^n\nabla D-\nabla P_{cwg}^n\right)C_2^{n+1}\right]\right\}+\hat{q}_wC_2^{n+1}=\phi^{(n+1)}\left[\left(c_w+c_\phi\right)S_w^nC_2^{n+1}\frac{\partial P_g}{\partial t}+\frac{\partial(S_wC_2)}{\partial t}\right] \tag{34}$$

$$\nabla\cdot\left\{k\lambda_w^n\left[\left(\nabla P_g^{(n+1)}-\gamma_w^n\nabla D-\nabla P_{cwg}^n\right)C_3^{n+1}\right]\right\}+\hat{q}_wC_3^{n+1}=\phi^{(n+1)}\left[\left(c_w+c_\phi\right)S_w^nC_3^{n+1}\frac{\partial P_g}{\partial t}+\frac{\partial(S_wC_3)}{\partial t}\right] \tag{35}$$

Implicit Pressure Implicit Saturation/Capillary Pressure Method

Global Pore Pressure Equation

$$\nabla\cdot\left\{k\lambda_t^n\left[\nabla P_g^{n+1}-\left(f_w\gamma_w+f_g\gamma_g\right)^n\nabla D-\left(f_w\nabla P_{cwg}\right)^n\right]\right\}+\hat{q_t}=\phi c_t\frac{\partial P_g}{\partial t}-\alpha_p\frac{\partial(\nabla\cdot\vec{u})}{\partial t}-(S_w^n\alpha_{T,w}+S_g^n\alpha_{T,g})\frac{\partial T}{\partial t} \tag{36}$$

Displacement Equation

$$G\nabla^2\vec{u}^{n+1}+(G+\lambda)\nabla(\nabla\cdot\vec{u}^{n+1})+\overrightarrow{\gamma_b}=-\alpha_p\left\{\nabla P_g^{n+1}-\left(f_w\gamma_w+f_g\gamma_g\right)^n\nabla D-\left(f_w\nabla P_{cwg}\right)^n\right\}-3\alpha_{T,b}K_b\nabla T^{n+1} \tag{37}$$

Temperature Equation

$$\begin{aligned}&\nabla\cdot(k_T\nabla T^{n+1})+\nabla\cdot\left\{k\lambda_t^n\left[\left(\rho_w c_{p,w}f_w^n+\rho_g c_{p,g}f_g^n\right)\nabla P_g^{n+1}-\left(\rho_w c_{p,w}f_w^n\gamma_w^n+\rho_g c_{p,g}f_g^n\gamma_g^n\right)\nabla D-\rho_w c_{p,w}f_w^n\nabla P_{cwg}^n\right]T^{n+1}\right\}\\&+\rho_i c_{p,i}\hat{q}_i(T_i-T_{ref})=\left\{\phi^n\left(\rho_w c_{p,w}S_w^n+\rho_g c_{p,g}S_g^n\right)+(1-\phi)\rho_s c_{p,s}\right\}\frac{\partial T}{\partial t}-3\alpha_{T,b}K_bT_{ref}\frac{\partial(\nabla\cdot\vec{u}\ )}{\partial t}\end{aligned} \tag{38}$$

Water Saturation Equation

$$\nabla\cdot\left\{k\lambda_w^n\left[\nabla P_g^{(n+1)}-\gamma_w^n\nabla D-\nabla P_{cwg}^{n+1}\right]\right\}+\hat{q}_w=\phi^{(n+1)}\left[\left(c_w+c_\phi\right)S_w^{n+1}\frac{\partial P_g}{\partial t}+\frac{\partial S_w}{\partial t}\right] \tag{39}$$

Concentration Equations

$$\nabla\cdot\left\{k\lambda_w^{(n+1)}\left[\left(\nabla P_g^{(n+1)}-\gamma_w^n\nabla D-\nabla P_{cwg}^{(n+1)}\right)C_1^{n+1}\right]\right\}+\hat{q}_wC_1^{n+1}=\phi^{(n+1)}\left[\left(c_w+c_\phi\right)S_w^{(n+1)}C_1^{n+1}\frac{\partial P_g}{\partial t}+\frac{\partial S_w}{\partial t}\right] \tag{40}$$

$$\nabla\cdot\left\{k\lambda_w^{(n+1)}\left[\left(\nabla P_g^{(n+1)}-\gamma_w^n\nabla D-\nabla P_{cwg}^{(n+1)}\right)C_2^{n+1}\right]\right\}+\hat{q}_wC_2^{n+1}=\phi^{(n+1)}\left[\left(c_w+c_\phi\right)S_w^{(n+1)}C_2^{n+1}\frac{\partial P_g}{\partial t}+\frac{\partial S_w}{\partial t}\right] \tag{41}$$

$$\nabla\cdot\left\{k\lambda_w^{(n+1)}\left[\left(\nabla P_g^{(n+1)}-\gamma_w^n\nabla D-\nabla P_{cwg}^{(n+1)}\right)C_3^{n+1}\right]\right\}+\hat{q}_wC_3^{n+1}=\phi^{(n+1)}\left[\left(c_w+c_\phi\right)S_w^{(n+1)}C_3^{n+1}\frac{\partial P_g}{\partial t}+\frac{\partial S_w}{\partial t}\right] \tag{42}$$

Numerical Discretization

To be consistent with commercial reservoir simulators, the finite-difference technique is chosen. Two different control volumes are used--one for fluid flow and another one for rock deformation. **Figure 6** shows how these two control volumes are staggered in each of the coordinate directions as well as the positions of the corresponding variables. As shown, for an arbitrary block, flow variables: pore pressure, temperature, fluid saturations and concentrations of three aqueous components are defined at the center of each grid block, while geomechanical variables: displacements are defined at the center of corresponding surface of each grid block.

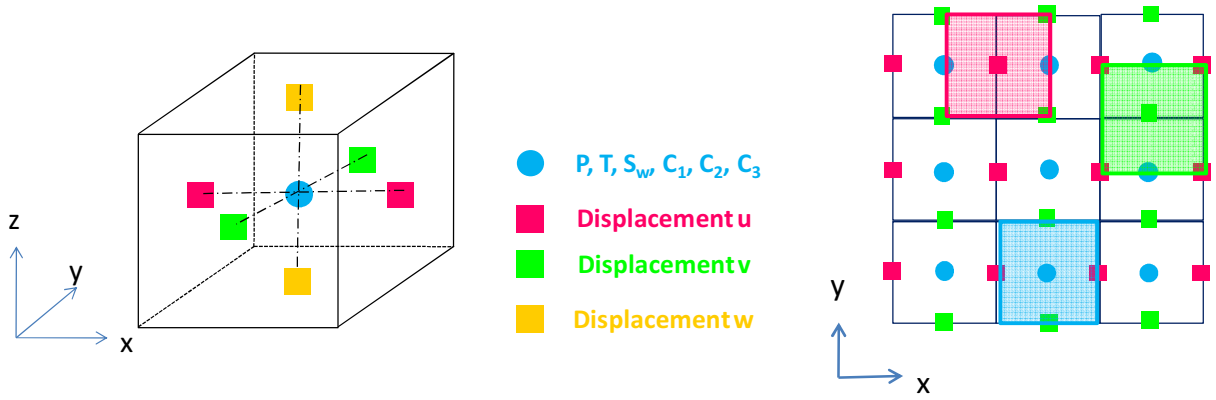

Figure 6. An arbitrary stagger grid block (left) and the positions and control volumes (represented by color-shaded rectangle) of variables in x-y plane (right).

The system of governing partial differential equations, Eqs.4-10 will be numerically discretized in both space and time. The spatial discretization will be handled with either one of finite-difference solution schemes (i.e. central-, forward- and backward- difference) to avoid matrix singularity problems. The time discretization will be carried out with a backward, first-order finite difference method. The final discrete nonlinear equations will be handled either by IMPES or implicit methods.

COUPLING PROCEDURE

The fracture module will be coupled with a reservoir module. During injection, the amount of fluid that leaks at each stage of fracture creation becomes a **source** term for the adjacent cell in the reservoir domain. During shut-in, fracture closure can be simulated from the fracture width equation (Eqs.2 and 3) coupled with reservoir module without source term. For fracture cleanup and production periods, the source term for the fracture cell connected to the well can be calculated based on specified bottom-hole pressure. The source terms are summarized below:

Source terms

For the reservoir cells adjacent to fracture cells

Injection: $q = \sum_{j=1}^{n} \frac{C_L A_{f,j}}{\sqrt{t_n - t_{j-1}}}$

Shut-in: $q = 0$

For the fracture cell connected to the well

Cleanup/Production: $q_k = -WI_k\left(P_{f(1,1,k)} - BHP\right)$ where $WI_k = 0.006328(k_f \lambda_t \Delta z)_k \frac{\bar{w}_{f,min}}{\frac{L_f}{2}}$

The coupling procedure is simply illustrated in **Figure 7.**

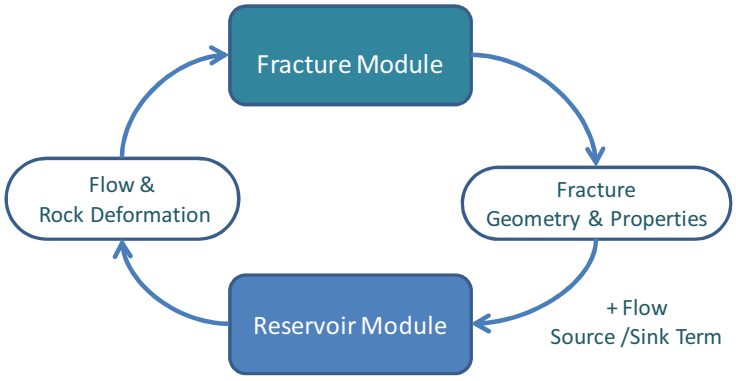

Period	Injection	Shut-in	Cleanup/ Production
Mechanism	Fracture Propagation & Leakoff	Fracture Closure & Leakoff	Production mode
Algorithm	Fracture Module & Reservoir Module	Fracture Module & Reservoir Module	Only Reservoir Module

Figure 7. Coupling procedure.

Preliminary Simulation Results

The first version of the geomechanics and flow model has been coded for water flooding as a test case of the geomechanical behavior. This code considers the effects of temperature, pore pressure, rock displacement, relative permeability, capillary pressure and gravity segregation in a reservoir-shale system. The 2-D preliminary results including pore pressure (P), temperature (T), water saturation (S_w), incremental displacements (U, W), porosity (ϕ), incremental normal and shear stresses ($\Delta\sigma_{xx}$, $\Delta\sigma_{zz}$, $\Delta\sigma_{xz}$). The simulation results are shown in **Figures 8** and **9**.

Initial conditions

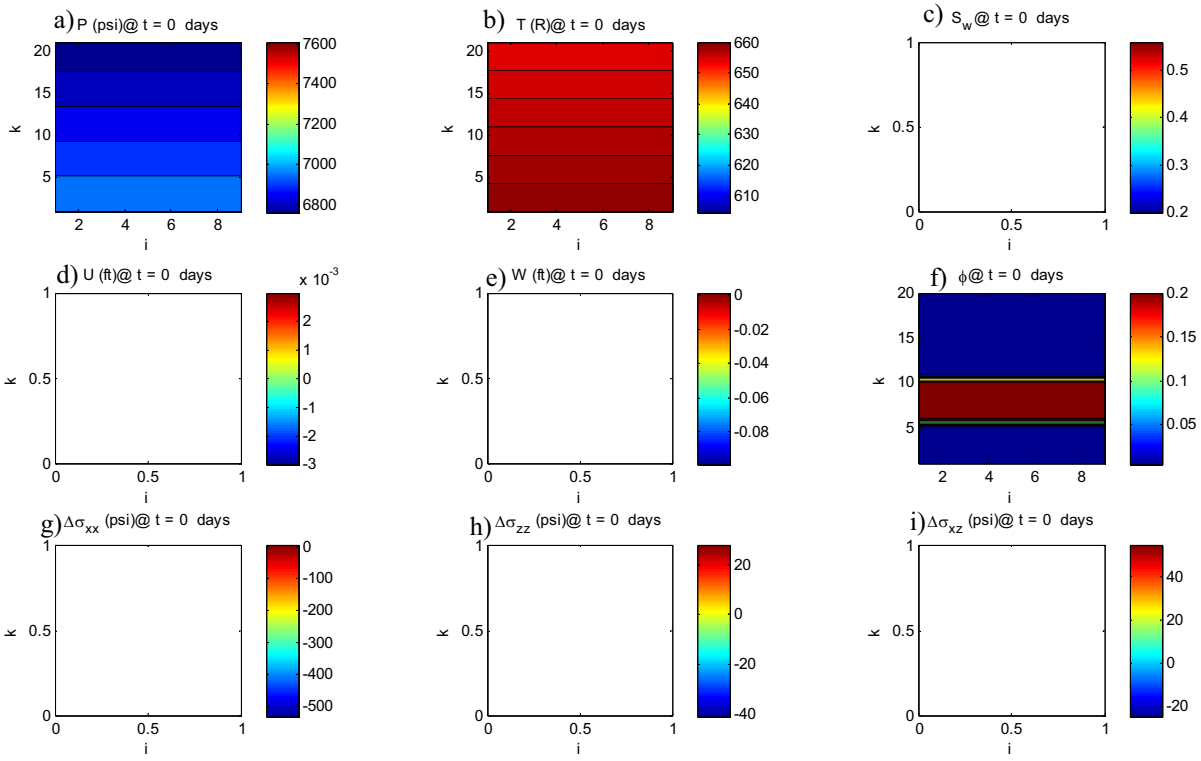

Figure 8. Contour plot of initial data in x-z plane where x- and y- axes are "i" and "k", which are grid indices in x- and z- directions, respectively. (a) pore pressure (b) temperature (c) water saturation, (d) incremental displacement in x-direction, (e) incremental displacement in z-direction, (f) matrix porosity, (g) incremental horizontal stress, (h) incremental vertical stress, and (i) incremental shear stress.

After waterflooding

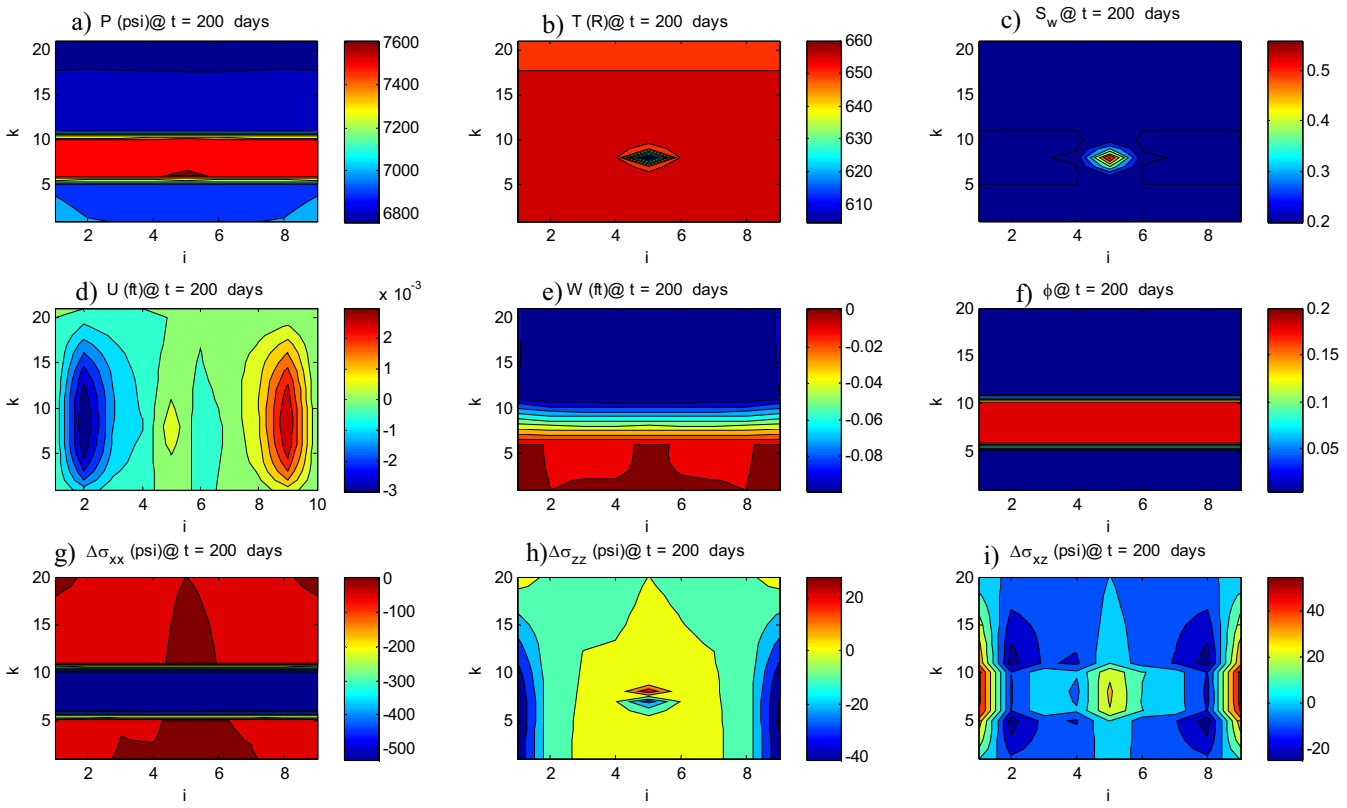

Figure 9. Contour plot of data after water flooding in x-z plane where x- and y- axes are "i" and "k", which are grid indices in x- and z- directions, respectively. (a) pore pressure (b) temperature (c) water saturation, (d) incremental displacement in x-direction, (e) incremental displacement in z-direction, (f) matrix porosity, (g) incremental horizontal stress, (h) incremental vertical stress, and (i) incremental shear stress.

NOMENCLATURE

A_f	fracture face area , L^2, ft^2, $A_f = L_f h_f$
A_{fj}	element j of the fracture face area, L^2, ft^2
$c_{p,s}$	isothermal heat capacity of rock, $L^2/(t^2\ T)$, Btu/(lb_m ^oR)
$c_{p,\varphi}$	isothermal heat capacity of phase φ, $L^2/(t^2\ T)$, Btu/(lb_m ^oR)
c_t	total system compressibility, Lt^2/m, psi^{-1}
c_φ	compressibility of phase φ, Lt^2/m, psi^{-1}
c_ϕ	pore compressibility, Lt^2/m, psi^{-1}
C_L	overall leakoff coefficient, $(L/t^{0.5})$, $(ft/min^{0.5})$
C_1	concentration of water, fraction
C_2	concentration of gel, fraction
C_3	concentration of gel breaker, fraction
D	depth measured from the datum point, L, ft
E	Young's modulus of rock, m/Lt^2, psi
f_φ	fractional flow of phase φ, dimensionless
G	shear modulus of rock, m/Lt^2, psi
h	formation thickness, L, ft
h_f	fracture height, L, ft
k	formation permeability, L^2, md
k_f	fracture or proppant permeability, L^2, md
$k_{r\varphi}$	relative permeability to phase φ, dimensionless
k_T	thermal conductivity of rock, $mL/(Tt^3)$, Btu/(ft ^oR day)
K_b	bulk modulus, m/Lt^2, psi
L_f	fracture half-length, L, ft
P	pore pressure or formation pressure, m/Lt^2, psi
P_{cwg}	water-gas capillary pressure, m/Lt^2, psi
P_f	fracture pressure, m/Lt^2, psi
P_φ	pore pressure of phase φ, m/Lt^2, psi
q_φ	source/sink term for phase φ, L^3/t, ft^3/d
q_i	well injection rate, L^3/t, ft^3/d
$\hat{q}$	sink/source term per volume of grid block, 1/t, 1/day
S_φ	saturation of phase φ, fraction
t	time, t, day
t	injection time, t, day (for Eq.1)
T	temperature, T, ^oR
T_{ref}	reference temperature, T, ^oR
$\vec{u}$	rock displacement vector
u	rock displacement (change from initial) element in x direction, L, ft
v	rock displacement (change from initial) element in y direction, L, ft
w	rock displacement element (change from initial) in z direction, L, ft
w_f	fracture width, L, ft
$\overline{w}_f$	average fracture width, L, ft
x	coordinate along fracture lateral propagation, distance in the x-direction, L, ft

y	coordinate perpendicular to fracture face, distance in the y-direction, L, ft
z	distance in the z-direction, L, ft
z	compressibility factor, dimensionless (for Eq.13)

Greek Letters

α_p	Biot's poroelastic constant or effective stress coefficient, dimensionless
$\alpha_{T,b}$	bulk coefficient of linear thermal expansion, 1/^{o}R
$\alpha_{T,s}$	coefficient of linear thermal expansion of rock, 1/^{o}R
$\alpha_{T,\varphi}$	coefficient of linear thermal expansion of phase φ, 1/^{o}R
γ_φ	gravity gradient of phase φ, m/L^{2}t^2, psi/ft, $\gamma_\varphi = \frac{\rho_\varphi}{144}$
Δ	change from initial
ΔL	grid length in x-direction, L, ft
Δt	time step size, t, day
$\overrightarrow{\Delta u}$	rock displacement (change from initial) vector, $\overrightarrow{\Delta u} = [u, v, w]^T$
Δx	grid length in x-direction, L, ft
Δy	grid length in y-direction, L, ft
Δz	grid length in z-direction, L, ft
δ_{ij}	Kronecker delta function ($\delta_{ij} = 1$ for $i = j$, $\delta_{ij} = 0$ for $i \neq j$)
ε	strain, dimensionless
ε_{ij}	strain components, dimensionless
ε_v	volumetric strain, dimensionless
λ	Lame's constant, m/Lt^2, psi
λ	time when the fluid has leaked from each small area element of a fracture or time when each small area element of a fracture is created or open to flow (for Eq.1)
λ_φ	mobility of phase φ, dimensionless
λ_t	total system mobility, dimensionless
μ_φ	viscosity of phase φ, m/Lt, cp
ρ_i	density of injection fluid, m/L^3, lb$_m$/ft^3
ρ_s	density of rock, m/L^3, lb$_m$/ft^3
ρ_φ	density of phase φ, m/L^3, lb$_m$/ft^3
σ_h	minimum horizontal stress, m/Lt^2, psi
σ_{ij}	stress components, m/Lt^2, psi
υ	Poisson's ratio of rock, dimensionless
ϕ	matrix porosity, fraction
ϕ_0	initial matrix porosity, fraction
ϕ_f	fracture or proppant porosity, fraction

Operator

∇	gradient operator
$\nabla \cdot$	divergence operator
∇^2	Laplacian operator

Superscript

n	current time level
$n+1$	next time level to be solved
$(n+1)$	next time level previously solved from the governing equations (pore pressure, displacement and temperature equations), which are known.

Subscript

b	bulk
f	fluid, fracture
g	gas
i	injection fluid
i, j, k	spatial coordinates x, y, z, respectively
max	maximum
min	minimum
n	last fracture segment
ref	reference
s	solid, grain
t	total, system
v	volumetric
w	water
x, y, z	x-, y-, z-directions, respectively
φ	fluid phase ($\varphi = g, w$ for gas, or water, respectively)
0	initial state

REFERENCES

1. Economides, M. J. and Martin, T. 2007. *Modern Fracturing: Enhancing Natural Gas Production.* Houston: ET Publishing.
2. Valko, P. and Economides, M.J. 1995. *Hydraulic Fracture Mechanics.* New York: John Wiley & Sons.
3. Wang, J. Y. 2008. Simulation of Fracture Fluid Cleanup and its Effect on Long-Term Recovery in Tight Gas Reservoirs. PhD dissertation, Texas A&M University, Texas.
4. Wills, H. A. 2009. 3D Numerical Investigation of Hydraulic Fracture Cleanup Processes. PhD dissertation, Colorado School of Mines, Golden, Colorado.
5. Carter, R.D. Derivation of the General Equation for Estimating the Extent of the Fractured Area, Appendix I of "Optimum Fluid Characteristics for Fracture Extension," *Drilling and Production Practice*, G.C. Howard and C.R. Fast, New York, New York, USA, American Petroleum Institute (1957), 261–269.
6. England, A.H. and Green, A.E. 1963. Some Two-Dimensional Punch and Crack Problems in Classical Elasticity. Proceedings of the Cambridge Philosophical Society, **59**(2):489-500.
7. Jaeger, J. C., Cook, N. G. W. and Zimmerman, R. W. 2007. *Fundamental of Rock Mechanics*. Oxford: Blackwell Publishing.
8. Chin, L.Y., Thomas, L.K., Sylte, J.E. and Pierson, R.G. 2002. Iterative Coupled Analysis of Geomechanics and Fluid Flow for Rock Compaction in Reservoir Simulation. *Oil&Gas Sci Tech—Rev.IFP*. **57** (5): 485-497.